Cosmic Research, Vol. 40, No. 3, 2002, pp. 241–254. Translated from Kosmicheskie Issledovaniya, Vol. 40, No. 3, 2002, pp. 261–275.

Shock–Acoustic Waves Generated during Rocket Launches and Earthquakes

E. L. Afraimovich, E. A. Kosogorov, and A. V. Plotnikov

Institute of Solar and Terrestrial Physics, Siberian Division, Russian Academy of Sciences, Irkutsk, 664033 Russia

Received May 31, 2000

Abstract—Shock–acoustic waves generated during rocket launches and earthquakes are investigated by a method developed earlier for processing data from a global network of receivers of the GPS navigation system. Disturbances of the total electron content in the ionosphere accompanying the launches of the *Proton*, *Soyuz*, and *Space Shuttle* space vehicles from the Baikonur cosmodrome and Kennedy Space Center launch site in 1998–2000, as well as the earthquakes in Turkey on August 17 and November 12, 1999, were analyzed. It was shown that, regardless of the source type, the impulsive disturbance has the character of an *N*-wave with a period of 200–360 s and an amplitude exceeding background fluctuations under moderate geomagnetic conditions by a factor of 2–5 as a minimum. The elevation angle of the disturbance wave vector varies from 25° to 65°, and the phase velocity (900–1200 m/s) approaches the speed of sound at heights of the ionospheric F-region maximum. The source location corresponds to a segment of the booster trajectories at a distance of no less than 500–1000 km from the start position and to a flight altitude of no less than 100 km. In the case of earthquakes the source location approximately coincides with the epicenter.

INTRODUCTION

A large number of publications [1–4] have been devoted to study of the ionospheric response to shock waves produced during rocket launches and earthquakes. Scientific interest in this problem is due to the fact that such cases can be considered as active experiments in the Earth's atmosphere, and they can be used in solving a wide variety of problems in ionospheric physics, radio wave propagation in the ionosphere, physics of atmospheric waves, etc. These investigations are also of practical importance since they help to validate reliable signal indications of both natural and technogenic effects (rocket launches, illegal explosions and underground nuclear tests, earthquakes). It is necessary to construct an effective global radiophysical system for the detection and localization of these effects. Essentially, existing global systems designed for this purpose use different processing techniques for infrasound and seismic signals. However, in connection with the expansion of geography and types of technogenic impact on the environment and due to its unpredictability, the problems of improving the sensitivity of detection and the reliability of the measured parameters of the sources of impacts, in particular, by involving independent measurements of the entire spectrum of signals generated during such effects, are still very urgent. Moreover, these investigations can prove to be useful for estimating possible consequences of the impact of rocket-and-space technology on the environment [5].

To solve these problems, one needs reliable information on basic parameters of the ionospheric response to a shock wave, such as its amplitude and form, the period, the phase and group velocity of the wave packet, and the angular characteristics of the wave vector. Note that terms allowing different physical interpretations are used in the literature for the ionospheric response to the shock wave. The term shock–acoustic wave (SAW) is one of them [6]. For notation convenience, we use this term in our paper, though it does not reflect the physical nature of the phenomenon completely.

It was often noted in the literature that the SAWs detected by the ionospheric soundings had a surprising similarity when generated during rocket launches, industrial explosions, and earthquakes. However, there is a large scatter of the data on the basic SAW parameters for all these events. The oscillation period of the ionospheric response to the SAW varied from 30 to 300 s; the velocity of propagation ranged from 700 to 1200 m/s [6–10].

The lack of comprehensive and reliable data on the SAW parameters is primarily due to limitations of the available experimental methods and detection facilities. Most data were obtained by measuring the Doppler frequency shift during vertical and tilt ionospheric soundings in the HF wave range [6, 9, 11]. In some cases, the sensitivity of this method is sufficient to detect the SAWs reliably; however, some difficulties arise with localization of the region of SAW generation, because of the multihop character of propagation of the HF wave signal.

Much of the experimental data on the SAW parameters were obtained from the methods of transionospheric sounding by measuring the Faraday rotation of the plane of signal polarization proportional to the total

0010-9525/02/4003-0241$27.00

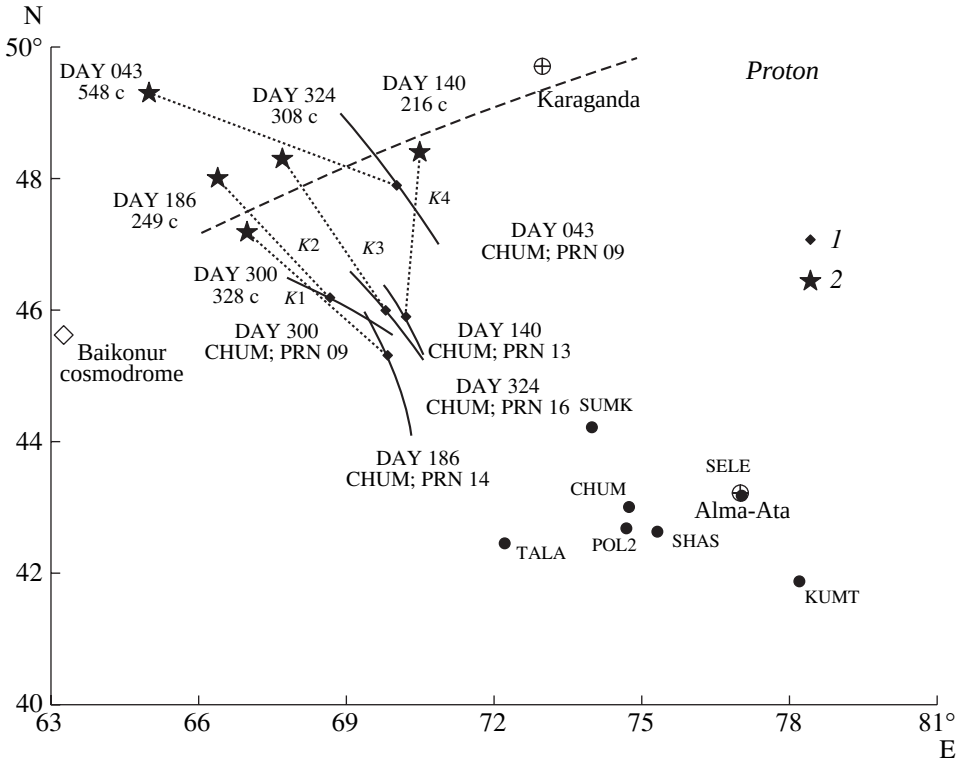

Fig. 1. The geometry of experiments during launches of the *Proton* launch vehicles from the Baikonur cosmodrome. The dashed line roughly corresponds to the horizontal projection of the rocket flight trajectory with an orbital inclination of 51.6°. The solid lines are for the trajectories of the subionospheric points for each GPS satellite at the altitude h_{max} = 400 km. The symbols (*1*) denote the position of the subionospheric points at the moment t_p of maximal TEC deviation. The symbols (*2*) show the source location at an altitude of 100 km as determined from the data of GPS-arrays. The numbers near the asterisks demonstrate the corresponding day number and the delay of the source "activation" with respect to the launch time. The straight dotted lines connecting the assumed source location and the subionospheric point represent the horizontal projection of the wave vector **K**. Heavy dots and uppercase letters mark the position and the names of the GPS stations, while lowercase letters along the trajectories refer to the station names and PRN numbers of the GPS satellites.

electron content (TEC) along the line connecting the satellite-borne transmitter with the receiver [12–14]. Ultra HF wave radio signals from geosynchronous satellites were applied in this case.

When the above-mentioned methods are used to define the SAW phase velocity, they suffer from one common drawback. It is necessary to know the time of the event in view, be it an industrial explosion, an earthquake, or a rocket launch, since this velocity is calculated from the SAW delay with respect to the time of the event under the assumption of constant velocity along the propagation path. This assumption does not correspond to reality.

To determine the above-indicated set of the SAW parameters, which is more or less complete, the appropriate spatial and temporal resolution is needed. However, the existing very sparse networks of ionosondes, tilt sounding radio paths, and incoherent scatter radars cannot provide such a resolution.

A new era in remote diagnostics of the ionosphere started after the development of the Global Positioning System (GPS) and the subsequent creation of widely branched networks of GPS stations on its basis. By February 2001, these networks contained more than 800 sites and their data were available via the Internet. This network will be considerably expanded in the near future due to its integration with the GLONASS navigation system [15]. Recently, scientists have started an intense development of methods of the GPS detection of the ionospheric response to strong earthquakes [1], rocket launches [16], and surface industrial explosions [7, 8]. The SAW phase velocity was defined in these studies by the "crossing" method, by estimating the delay of the SAW arrival at subionospheric points, which correspond to different GPS satellites observed at that moment. However, the accuracy of this method is rather low because the altitude at which the subionospheric points are specified is determined approximately.

In [17, 18], a method was developed for determining SAW parameters (including the phase velocity, angular characteristics of the SAW wave vector, the direction towards the source, and the source location) with the use of GPS-arrays, the elements of which could be chosen from a large set of GPS stations of the global GPS

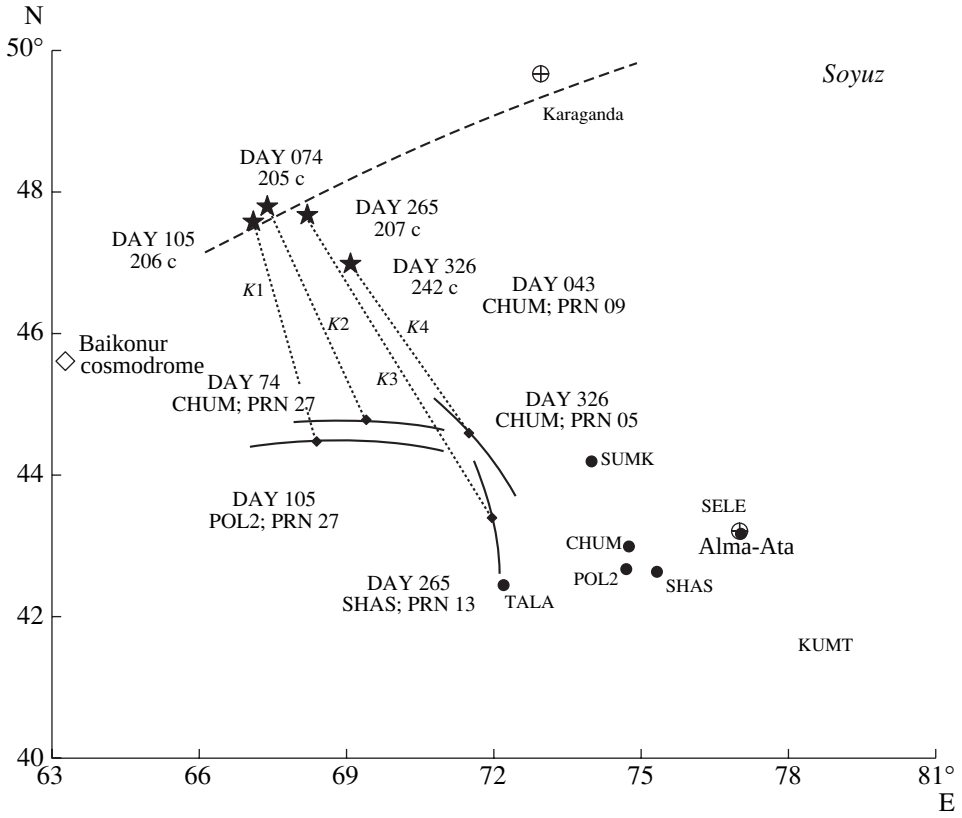

Fig. 2. The geometry of experiments during launches of the *Soyuz* launch vehicles from the Baikonur cosmodrome. The notation is the same as for Fig. 1.

network. Unlike the well-known radiophysical methods, this one provides an estimate of the SAW parameters without a priori information about the location and time of the event (rocket launches, explosions, earthquakes).

The goal of this paper is to investigate the shock–acoustic waves generated during rocket launches and earthquakes. Section 2 presents the geometry of the experiments. A brief description of the method applied [17, 18] is given in Section 3. Measurements of the SAW parameters for different GPS-arrays during rocket launches and earthquakes are presented in Section 4. The experimental results are discussed in Section 5.

2. GEOMETRY OF THE EXPERIMENTS

The basic parameters are determined and presented in this paper for the SAWs following the launches of the *Proton* and *Soyuz* boosters from the Baikonur cosmodrome (45.6°N, 63.3°E) and the launches of the *Space Shuttle* launch vehicles (LVs) from the Kennedy Space Center (KSC, 28.5°N, 279.3°E0) in 1998–2000 (11 launches in all). In addition, similar investigations were performed for two earthquakes in Turkey, on August 17 and November 12, 1999.

Though the number of GPS stations is large, one encounters some difficulties in selecting GPS-arrays for the detection of SAWs generated during rocket launches as for both cosmodromes the LV flight paths lie either over the Atlantic Ocean (for the *Space Shuttle* LV) or over underpopulated regions of Kazakhstan (for the *Proton* and *Soyuz* LVs). A low density of GPS stations is also typical of Turkey. Nevertheless, we managed to use enough GPS stations so that their number was sufficient to implement the method suggested.

The geometry of experiments performed during the *Proton* and *Soyuz* LVs launches from the Baikonur cosmodrome is sketched in Figs. 1 and 2. The dashed line roughly corresponds to the horizontal projection of the rocket flight trajectory with an orbital inclination ψ = 51.6° (http://www.ilslaunch.com). The station coordinates are not given here because of space limitations; they can be found at the Internet site http://lox.ucsd.edu. The coordinate axes are scaled so that the linear dimensions along latitude and longitude are approximately the same.

The geometry of the experiments during the launch of a *Space Shuttle* from the KSC is presented in Fig. 3. The *Space Shuttle Columbia* lifted off on mission STS-95 from the KSC launch site on October 29, 1998 (Day 302).

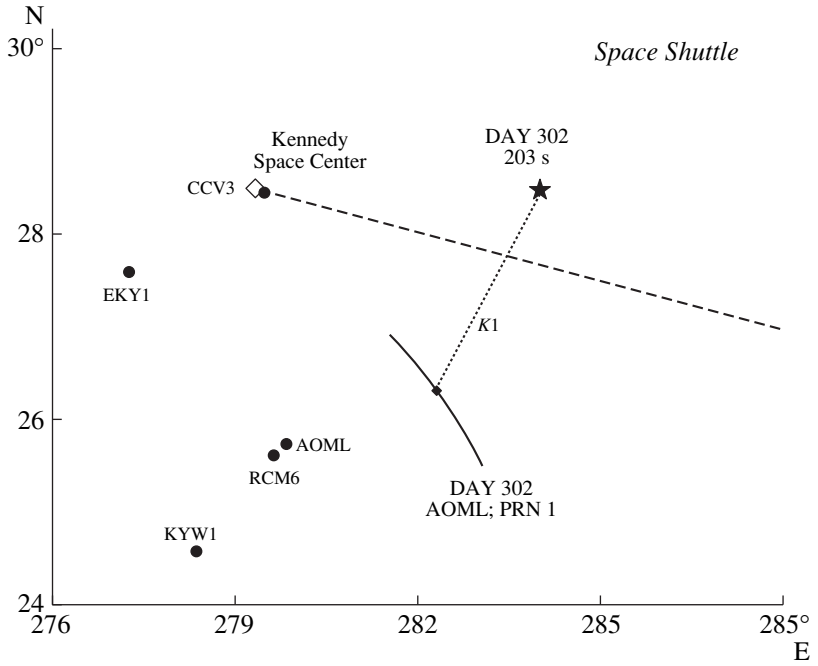

Fig. 3. The geometry of experiments during launches of the *Space Shuttle* (STS-95) launch vehicles from the Kennedy Space Center.

The following information about rocket launches from the Baikonur cosmodrome and the KSC is extracted from the Internet sites http://www.flatoday.com and http://www.spacelaunchnews.com. General information on these launches is summarized in Table 1 (including the launch time t_0, in the universal time UT; the number of the day in a year; the orbital inclination; and the level of geomagnetic disturbance from the data on D_{st} variations). It was found that the deviation of D_{st} was quite moderate for the selected days; thus, the SAWs could be identified reliably.

Table 1. General information about rocket launches

Type	Date	t_0, UT	ψ, deg	D_{st}, nT
Proton	November 20,1998 (DAY 324)	06:40	51.6	−9
Proton	May 20, 1999 (DAY 140)	22:30	51.6	−3
Proton	July 5, 1999 (DAY 186)	13:32	51.6	+11
Proton	October 27, 1999 (DAY 300)	16:16	51.6	−80
Proton	February 12, 1999 (DAY 74)	09:10	51.6	−108
Soyuz	March 15, 1999 (DAY 74)	03:06	51.6	−16
Soyuz	April 15, 1999 (DAY 105)	00:46	51.6	−3
Soyuz	September 22, 1999 (DAY 265)	14:33	51.6	+22
Soyuz	November 22, 1999 (DAY 326)	16:20	51.6	−25
Shuttle	April 17, 1998 (DAY 107)	18:19	39	−37
Shuttle	October 29, 1998 (DAY 302)	19:19	28.5	−15

The experimental geometry during the earthquakes in Turkey on August 17 and November 12, 1999, is sketched in Fig. 4. The information given below on the earthquakes was acquired via the Internet from the site http://earthquake.usgs.gov. General information about these earthquakes is presented in Table 2 (including the time of the main shock t_0, in the universal time UT; the position of the earthquake epicenter; its depth and magnitude, as well as the level of geomagnetic disturbance obtained from the data on D_{st} variations). It turned out that, as in the case of rocket launches, the deviation of D_{st} variations was quite moderate for the days of interest; thus, the SAWs could be identified reliably.

3. DETERMINATION OF THE CHARACTERISTICS OF SHOCK–ACOUSTIC WAVES

The standard GPS technology provides a means for detection of wave disturbances in the ionosphere on the basis of phase measurements of the total electron content (TEC) I [1, 7, 16, 19]:

$$I = \frac{1}{40.308}\frac{f_1^2 f_2^2}{f_1^2 - f_2^2}[(L_1\lambda_1 - L_1\lambda_2) + \text{const} + nL], \quad (1)$$

where $L_1\lambda_1$ and $L_2\lambda_2$ are the increments of the phase path of the radio signal due to the phase delay in the

ionosphere (m); L_1, L_2 are the number of phase rotations; and λ_1, λ_2 are the wavelengths (m) for the frequencies f_1 and f_2; const is an unknown initial phase path (m); and nL is the error in the phase path determination (m).

Phase measurements in the GPS are performed with a high accuracy corresponding to the errors of TEC determination of less than 10^{14} m^{-2} for 30-s intervals of averaging, though the initial value of the TEC is unknown [19]. This allows ionization irregularities and wave processes to be detected in the ionosphere over a wide range of amplitudes (up to 10^{-4} of the diurnal TEC variation) and periods (from 24 h to 5 min). Henceforth, we use the unit of TEC generally accepted in literature, TECU, which is equal to 10^{16} m^{-2}.

In some cases, the calculation of Doppler frequency shifts F from the TEC series obtained by formula (1) is the most convenient way of detecting the ionospheric response to a shock wave and determining its delay. Such an approach is also useful when we compare the characteristics of TEC response obtained from the GPS data to those obtained by analyzing ultra HF wave signals from geosynchronous satellites, as well as by detecting the shock wave in the HF wave range. To an approximation sufficient for the purpose of our investigation, the corresponding relationship was obtained [20]:

$$F = 13.5 \times 10^{-8} I_t' / f, \qquad (2)$$

where I_t' stands for the time derivative of the TEC. The relevant results derived from analyzing the $F(t)$ variations calculated for the "reduced" frequency of 136 MHz are discussed in Section 4.

An agreement between space-and-time phase characteristics obtained by transionospheric soundings in the plane of the antenna system and local characteristics of ionospheric disturbances has been considered in detail in a variety of publications [9, 21–23] and is not analyzed in our study. The most important conclusion made in the above-cited papers is that, as in an extensively used model of a "plane phase screen," the TEC disturbances $\Delta I(x, y, t)$ detected by the transionospheric soundings are perfectly similar to the horizontal part of the corresponding local disturbance of the electron density $\Delta N(x, y, z, t)$ and can be used in experiments on measuring the azimuth of propagation of the wave disturbances of the TEC.

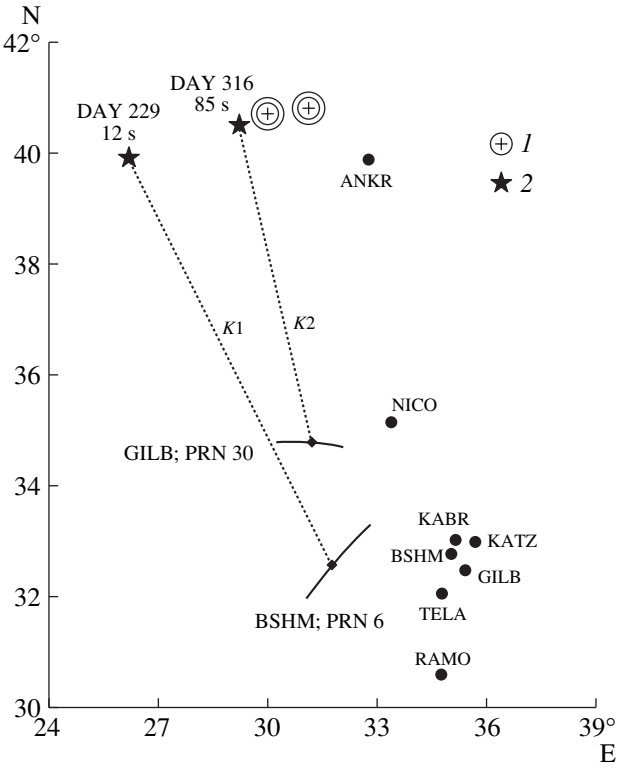

Fig. 4. Experimental geometry during the earthquakes in Turkey on August 17 and November 12, 1999. (*1*) The positions of the earthquake epicenters; (*2*) the source location at the ground level as determined from the GPS-array data.

However, the amplitude of the TEC response experiences a strong aspect-angle dependence caused by the integral character of the transionospheric sounding. The maximal response is associated with the wave disturbances whose wave vector $\mathbf{K}_t$ is perpendicular to the direction $\mathbf{r}$ towards the GPS satellite. The condition for the elevation θ and azimuth α angles of an arbitrary wave vector $\mathbf{K}_t$ normal to the direction $\mathbf{r}$ has the following form:

$$\theta = \arctan(-\cos(\alpha_s - \alpha)/\tan\theta_s), \qquad (3)$$

where θ_s and α_s are the elevation angle and azimuth of the vector $\mathbf{r}$. We use formula (3) to determine the elevation angle θ of the wave disturbance vector $\mathbf{K}_t$ from the known azimuth α.

We determine the velocity and the direction of displacement of the phase front within the framework of some model describing these phenomena. An adequate

Table 2. General information about the earthquakes in Turkey

Epicenter	Date	t_0, UT	Depth, km	Magnitude, mb Ms Mw	D_{st}, nT
40.70°N, 29.99°E	August 17, 1999 (DAY 229)	00:00:39	17	6.3 7.8 7.4	–14
40.79°N, 31.11°E	November 12, 1999 (DAY 316)	16:57:20	10	6.5 7.5 7.1	–44

choice of the model is crucial. In the simplest form, the space-and-time TEC variations at each given moment t can be presented in the form of a solitary plane traveling wave [24]:

$$\Delta I(t, x, y) = \delta \sin(\Omega t - K_x x - K_y y - \varphi_0), \qquad (4)$$

where δ, K_x, K_y, Ω are the amplitude, x- and y-components of the wave vector $\mathbf{K}$, and the angular frequency of the disturbance, respectively; $T = 2\pi/\Omega$ and $\Lambda = 2\pi/|K|$ are its period and wavelength, respectively; and φ_0 is the initial phase of the disturbance. The vector $\mathbf{K}$ is the horizontal projection of the total vector $\mathbf{K}_t$.

Here we assume that the influence of second derivatives can be neglected if the space-and-time increments are small (the distances between the sites in the GPS-array are less than the typical spatial scale of the TEC variations, and the time interval between counts is less than the corresponding time scale). All of the following choices of GPS-arrays meet these requirements.

Let us briefly present the sequence of data processing procedures. Three sites (A, B, and C) are selected out of a large number of GPS stations so that the distances between them do not exceed about half of the expected wavelength Λ of the disturbance. Site B is taken as the center of a topocentric frame of reference with the x axis directed eastward and the y axis directed northward. In this frame of reference the receivers have the coordinates $S(x_A, y_A)$, $b(0, 0)$, and $C(x_C, y_C)$. This configuration of the GPS receivers represents a GPS-array with a minimal required number of elements. In the regions with a dense network of GPS sites, we can obtain a series of GPS-arrays with different configurations. This provides for the possibility to test the reliability of the data obtained; we use this possibility in the present paper.

The input data include series of the "oblique" TEC values $I_A(t)$, $I_B(t)$, $I_C(t)$ and the corresponding series of elevation angles $\theta_s(t)$ and azimuths $\alpha_s(t)$ of the beam to the satellite calculated with the help of the CONVTEC code, which we developed to convert the RINEX-files, standard for the GPS system, obtained via the Internet. To determine the SAW characteristics we selected continuous series of measurements of $I_A(t)$, $I_B(t)$, and $I_C(t)$ with lengths greater than one hour including the time of the event.

To eliminate variations of the regular ionosphere, as well as the trends introduced by the orbital motion of a satellite, we applied a procedure of trend removal involving preliminary smoothing of the initial series with a selected time window. This procedure is better suited to discrimination of such a signal as a single pulse (N-wave) than the frequently used bandpass filter [1, 7, 8, 14, 16]. The limitations of the bandpass filter are a delay and an oscillatory character of the response, which does not allow one to reconstruct the form of the N-wave accurately.

The series of elevation angles $\theta_s(t)$ and azimuths $\alpha_s(t)$ of the beam to a satellite are used to determine the coordinates of the subionospheric point and to calculate the elevation angle θ of the wave vector $\mathbf{K}_t$ of the disturbance from the known azimuth α (formula (3)).

The determined SAW parameters are most reliable at high values of elevation angles $\theta_s(t)$ of the beam to the satellite, because sphericity effects become reasonably small in this case. In addition, there is no need to convert the "oblique" value of TEC $I(t)$ to the "vertical" one. All results of this study were obtained for the elevation angles $\theta_s(t)$ larger than 30°.

Since the distance between the elements of the GPS-array (from several hundred to a few thousand kilometers) is much smaller than that to the GPS satellite (more than 20 000 km), the array geometry at the height of the subionospheric point $h_{\max}$ (about 400 km) is identical to that at the Earth's surface.

Figure 5 shows typical time dependences of the "oblique" TEC $I(t)$ at one of three sites of the GPS-array near the Baikonur cosmodrome for the launch days (thick line), one day before and after the launches (thin lines), for the missions of *Proton* on July 5, 1999 (panel *a*), and *Soyuz* on April 15, 1999 (panel *d*). Panels *b* and *e* show TEC variations $\Delta I(t)$ for the same days but with the removed linear trend and smoothed with a 5-min time window. Panels *c* and *f* present variations in the Doppler shift of frequency $F(t)$ "reduced" to the sounding frequency of 136 MHz for three sites of the array for the launch days. The day numbers, names of GPS stations, and PRN numbers of GPS satellites are included in all panels. The arrows at the x axis indicate the launch time t_0.

It is evident from Fig. 5b that fast N-shaped oscillations with a typical period T of about 300 s, which are induced by the SAW propagation, are clearly distinguished among slow TEC variations. The oscillation amplitude (about 0.5 TECU) is much greater than the intensity of TEC fluctuations on "background" days. Variations in the Doppler shift of frequency $F(t)$ (Fig. 5c) for spatially separated sites (SELE, CHUM, SHAS) are well correlated.

Taking into account a good signal/noise ratio (better than 1), the horizontal projection of the phase velocity V_h for the given coordinates of the array sites A, B, and C is determined from the relative temporal shifts t_p of the time of maximal TEC deviation. Preliminarily measured shifts are subjected to a linear transformation in order to calculate shifts for the sites spaced northward V_x and eastward V_y relative to the central site. This is followed by calculation of the E- and N-components of V_x and V_y, as well as the direction α in the range of angles 0°–360° and the magnitude V_h of the horizontal component of the SAW phase velocity:

$$\alpha = \arctan(V_y/V_x),$$
$$V_h = |V_x V_y|(V_x^2 + V_y^2)^{-1/2}, \qquad (5)$$

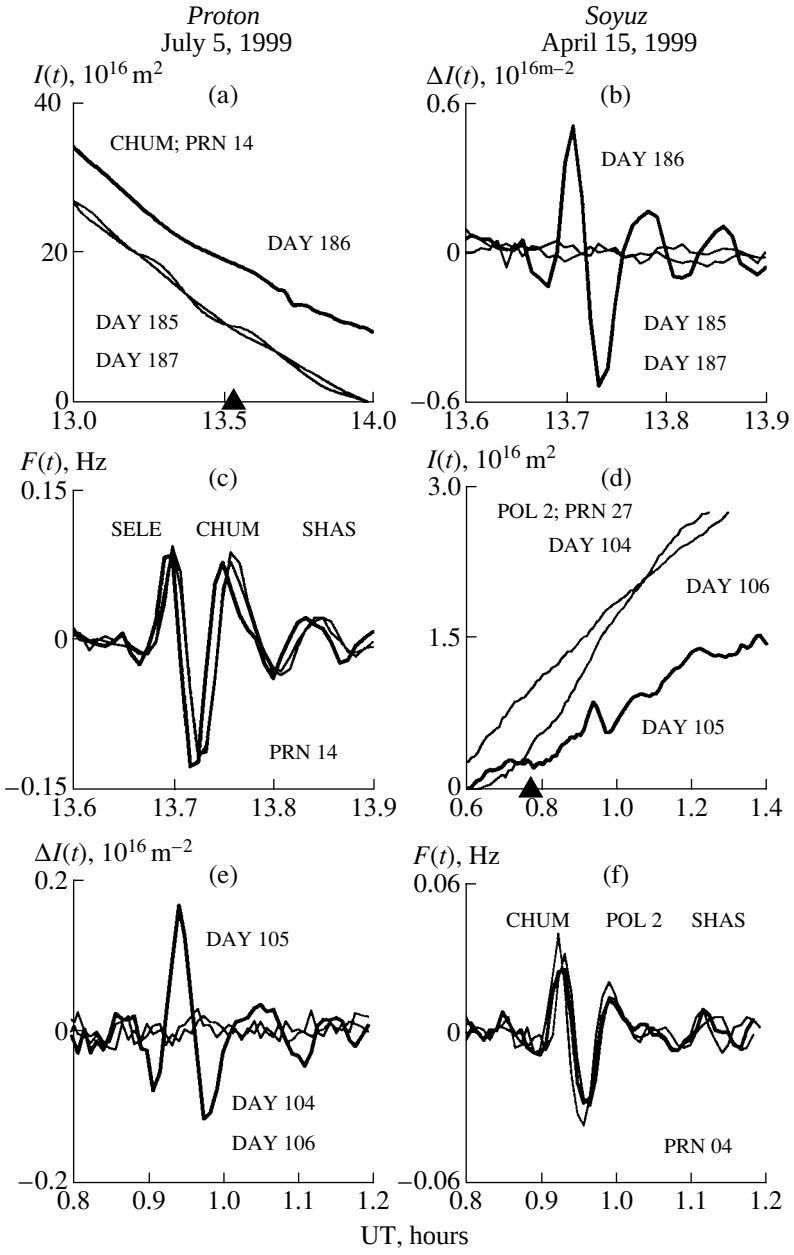

Fig. 5. Time dependences of the "oblique" TEC $I(t)$.

where V_y and V_x are the velocities with which the phase front crosses the axes x and y. The orientation α of the wave vector **K**, which is coincident with the propagation azimuth of the SAW phase front, is calculated unambiguously in the range 0°–360°, subject to the condition that ($\arctan(V_y/V_x)$ is calculated with regard to the sign of the numerator and denominator.

The above method for determining the SAW phase velocity neglects a correction for the orbital motion of the satellite, because the estimates of V_h obtained below exceed the velocity of the subionospheric point at the height h_{max} and elevation angles $\theta_s > 30°$ [24] by an order of magnitude, as a minimum.

In order to compare our estimates of the SAW phase velocity with those obtained by the method generally used to measure this quantity, we also calculated the SAW mean velocity V_a from the delay $\Delta t = t_p - t_0$ and the known path length between the launch site and the subionospheric point.

It was shown in [22] that for the Gaussian model of ionization distribution, the amplitude M of the TEC disturbance is determined by the aspect angle γ between the vectors $\mathbf{K}_t$ and **r** and by the ratio of the wavelength

of the disturbance Λ to the half-thickness of the ionization maximum h_d:

$$M \propto \exp\left(-\frac{\pi^2 h_d^2 \cos^2\gamma}{\Lambda^2 \cos^2\theta_s}\right). \quad (6)$$

In our case (see below), for the phase velocity of about 1 km/s and for the period of about 200 s, the wavelength Λ proves to be comparable with the half-thickness of the ionization maximum h_d. At the elevation angles θ_s equal to 30°, 45°, and 60° a half-power "beamwidth" $M(\gamma)$ is 25°, 22°, and 15°, respectively. If h_d is twice as large as the wavelength Λ, then the beamwidth tapers to 14°, 10°, and 8°, respectively.

The beamwidth is sufficiently small; thus, the aspect condition (3) restricts the number of beam trajectories to the satellite for which a reliable detection of the SAW response is possible in the presence of the background noise (for angles of about $\gamma = 90°$).On the other hand, formula (3) can be used to determine the elevation angle θ of the wave vector $\mathbf{K}_t$ of the shock wave for a given value of the azimuth α [24]. Then, the magnitude of the phase velocity V_t can be determined as

$$V_t = V_h \cos(\theta). \quad (7)$$

The above values of the width $M(\gamma)$ determine the error of calculating the elevation angles θ (on the order of 20° for the indicated conditions) and, as a consequence, of the coordinates of the assumed source (see below).

The ionospheric region that is responsible for the main contribution to TEC variations lies near the maximum of the ionospheric F-region, thus defining the height F of the subionospheric point. When selecting $h_{\max}$, it should be taken into account that above the main maximum of the F2-layer the electron density decreases with height much more slowly than below this maximum. Since the vertical density distribution is essentially a "weight function" of the TEC response to a wave disturbance [22], the value exceeding the true height of the layer maximum h_{F_2} by about 100 km is reasonably used as $h_{\max}$. The value of h_{F_2} varies in a wide range (250–350 km) depending on the time of day and on some geophysical factors, which, when necessary, can be taken into account if the corresponding additional experimental data and state-of-the-art ionospheric models are applied. Hereafter, we assumed $h_{\max} = 400$ km in all calculations.

To a first approximation, it can be assumed that an imaginary detector, which records the ionospheric SAW response in TEC variations, is located just at this altitude. "The horizontal extent" of the detection region, which can be estimated from the velocity of displacement of the subionospheric point due to the GPS satellite motion (on the order of 70–150 m/s) and from the SAW period (of about 200 s; see Section 4), does not exceed 20–40 km, being essentially smaller than its "vertical extent".

From GPS data we can determine the coordinates X_s and Y_s of the subionospheric point in the horizontal plane $X0Y$ of the topocentric frame of reference centered at the site $B(0, 0)$ at the time of maximal TEC deviation caused by the SAW arrival at this point. Since we know the angular coordinates θ and α of the wave vector $\mathbf{K}_t$, we can find the coordinates of the point at which this vector intersects the horizontal plane $X'0Y'$ at the height h_ω of the assumed source. Assuming a rectilinear propagation of the SAW from the source to the subionospheric point and neglecting the Earth's sphericity, the coordinates X_ω and Y_ω of the source in the topocentric frame of reference can be defined as

$$X_\omega = X_p - (h_{\max} - h_\omega)\frac{\cos\theta\sin\theta}{\sin\theta}, \quad (8)$$

$$Y_\omega = Y_p - (h_{\max} - h_\omega)\frac{\cos\theta\cos\theta}{\sin\theta}. \quad (9)$$

The coordinates X_ω and Y_ω obtained in this way can be easily converted to the values of latitude and longitude (ϕ_ω and λ_ω) of the source.

For SAWs generated during earthquakes, industrial explosions, and underground tests of nuclear devices, h_ω is taken equal to 0 (the source is at ground level). When we record the SAWs produced by launches of powerful rockets, the region of SAW generation can lie at heights h_ω of about 100 km or higher [14, 25].

In this approximation we neglect a possible refraction arising during the SAW propagation from the source to the height $h_{\max}$. In some papers [8] this problem is solved by performing trajectory calculations with the use of standard "ray tracing" procedures and models of the neutral atmosphere. In this case, the ray trajectories are calculated starting from the source. We also can perform such calculations starting not from the source but from the subionospheric point (a backtraced trajectory).

Given the coordinates of the subionospheric point and those of the disturbance source, the mean value of the SAW propagation velocity along the path from the source to the subionospheric point, and the time of the SAW arrival at this point, the delay Δt_ω of "activation" of the assumed SAW source with respect to the time of the event can easily be estimated under the assumption of rectilinear propagation. The estimates of Δt_ω given below assume that the propagation velocity is 700 m/s [7, 14]. Note that by the time of the source "activation," we mean the moment of the maximal disturbance of the background state of the medium during the SAW generation.

Table 3. *Proton* and *Soyuz* launches from the Baikonur cosmodrome

T, s	A_I, TECU	A_F, Hz	θ, deg	α, deg	V_h, m/s	V_t, m/s	V_α, m/s	λ_ω, deg	φ_ω, deg	Δt_ω, s
Proton, November 20, 1998										
300	0.09	0.022	52.8	163	1338	809	890	48.3	67.7	308
Proton, May 20, 1999										
340	0.05	0.01	35.4	166	1556	1261	740	48.4	70.5	216
Proton, July 5, 1999										
305	0.5	0.13	57.3	157	1882	1005	966	48.0	66.4	249
Proton, October 27, 1999										
285	0.08	0.02	47.8	158	1673	1125	791	47.2	67.0	328
Proton, February 12, 2000										
260	0.034	0.012	65.0	158	1461	616	616	49.3	65.0	548
Soyuz, March 15, 1999										
306	0.2	0.04	41.5	160	1733	1251	1017	47.8	67.4	205
Soyuz, April 15, 1999										
295	0.2	0.043	41.7	166	1627	1200	818	47.6	67.1	206
Soyuz, September 22, 1999										
275	0.05	0.01	28.6	150	1078	945	880	47.7	68.2	207
Soyuz, November 22, 1999										
276	0.03	0.008	38.3	140	1240	972	966	47.0	69.1	242

4. MEASUREMENT RESULTS

Thus, applying the transformations described in Section 3, we derived from TEC variations the following parameters, which characterize the SAWs: t_p, the time of maximal TEC deviation; Δt, the delay of t_p with respect to t_0; T, the SAW period; A_I, the amplitude of the TEC disturbance; A_F, the amplitude of the maximum Doppler frequency shift at the "reduced" frequency of 136 MHz; α and θ, the azimuth and elevation angles of the wave vector $\mathbf{K}_t$; V_h and V_t, the horizontal component and magnitude of the phase velocity; V_a, the average wave velocity as calculated from the delay Δt and the known path length between the epicenter of an earthquake or the launch site and the subionospheric point; ϕ_ω and λ_ω, the latitude and longitude of the source at ground level for earthquakes and at an altitude of 100 km for rocket launches; and Δt_ω, the delay of the "activation" of the assumed SAW source with respect to the time of the event.

It should be noted that the estimates of A_I and A_F were obtained from the filtered series of the "oblique" TEC values. Therefore, the equivalent estimates for the "vertical" TEC are smaller by a factor varying from 1 to 2 with the elevation angle θ_s of the beam to the satellite.

To verify the reliability of the determined basic parameters of the SAW form and dynamics for the events considered, we chose different combinations of three sites from available sets of GPS stations and processed these data with identical processing parameters. The corresponding mean values of these variables are given in Tables 3 and 4 and in Figs. 1–4 (the location of the SAW source).

Solid curves in Figs. 1–4 show the trajectories of subionospheric points for each GPS satellite at the height h_{max} = 400 km. Dark diamonds along the trajectories mark the coordinates of subionospheric points at the moments t_p of maximal TEC deviations. Asterisks designate the location of the SAW sources as determined from the GPS-array data. Numbers at the asterisks refer to the corresponding day numbers. Dotted straight lines connecting the assumed source with the subionospheric point show the horizontal projections of the corresponding wave vectors $\mathbf{K}_t$.

Let us consider the results of analyzing the ionospheric effect of SAWs during the *Proton* launch on July 5, 1999, obtained at the array (SELE, CHUM, SHAS) for PRN14 (on the left of Fig. 5).

In this case, the delay of the SAW response with respect to the launch time is 12 min. The SAW has the form of an *N*-wave with a period T of about 300 s and an amplitude A_I = 0.5 TECU, which is an order of magnitude larger than TEC fluctuations on background days. The considered time interval is characterized by a very low level of geomagnetic activity (11 nT).

The amplitude of maximal Doppler shift of frequency A_F at the "reduced" frequency of 136 MHz was found to be 0.12 Hz. In view of the fact that the shift F is inversely proportional to the squared sounding frequency [20], this corresponds to a Doppler shift of about A_F = 12 Hz at the

Table 4. *Shuttle* launches and the earthquakes in Turkey

T, s	A_I, TECU	A_F, Hz	θ, deg	α, deg	V_h, m/s	V_t, m/s	V_α, m/s	λ_ω, deg	φ_ω, deg	Δt_ω, s
Shuttle, April 17, 1998										
263	0.57	0.16	30.5	140	3590	3094	1255	36.9	284	–
Shuttle, October 29, 1999										
218	0.27	0.05	34.4	214	1529	1263	734	28.6	284	203
Turkey, August 17, 1999										
354	0.14	0.04	24.1	156	1286	1173	870	39.9	26.2	12
Turkey, November 12, 1999										
195	0.079	0.023	37.6	186	1478	1157	812	40.5	29.2	85

working frequency of 13.6 MHz for the equivalent tilt sounding path.

The azimuth α and elevation angle θ of the wave vector $\mathbf{K}_t$ whose horizontal projection is shown in Fig. 1 by the dotted line marked by $\mathbf{K}_1$ are 153° and 59°, respectively. The horizontal component and the magnitude of the phase velocity turned out to be V_h = 1808 m/s and V_t = 931 m/s. The source coordinates at an altitude of 100 km were determined as ϕ_ω = 48° and λ_ω = 66°. The delay of "activation" of the SAW source Δt_ω with respect to the launch time was 264 s.

Similar results were also obtained at the array (CHUM, POL2, SHAS) and PRN27 for the launch of *Soyuz* LV on April 15, 1999. They correspond to the projection of the vector $\mathbf{K}_1$ in Fig. 2 and to the time dependences in Fig. 5.

A comparison of data for other standard launches of the *Proton* and *Soyuz* LVs (Table 3, average values are presented) demonstrated that the SAW parameters agree well, regardless of the rocket type, the level of geomagnetic disturbance, the season, and the local time. The small scatter of coordinates of the SAW sources as determined in this study (see Table 3; Figs. 1, 2) is also significant. It should be noted that the wave vector **K** proved to be nearly perpendicular to the direction of the horizontal projection of the LV trajectories for all LV launches from the Baikonur cosmodrome.

Let us consider the results of analyzing the ionospheric effect of SAWs during the *Space Shuttle* launch on October 29, 1998 (Table 4), obtained at the array (AOML, KYW1, EKY1) for PRN01 (Fig. 6).

As in the case of the *Proton* LV launches, the delay of the SAW response with respect to the launch time is 12 min. The SAW has the form of an *N*-wave with a period T of about 210 s and an amplitude A_I = 0.3 TECU, which is an order of magnitude larger than the TEC fluctuations on background days. The amplitude of the maximal Doppler frequency shift A_F at the "reduced" frequency of 136 MHz was found to be 0.07 Hz.

The azimuth α and elevation angle θ of the wave vector $\mathbf{K}_t$ whose horizontal projection is shown in Fig. 3 by the dotted line marked by $\mathbf{K}_1$ are 214° and 34.6°, respectively. The horizontal component and the magnitude of the phase velocity turned out to be V_h = 1502 m/s and V_t = 1235 m/s. These values are close to those for the *Proton* and *Soyuz* LVs. The source coordinates at an altitude of 100 km were determined as ϕ_ω = 27.4° and λ_ω = 283°. The delay of "activation" of the SAW source Δt_ω with respect to the launch time was 200 s.

Similar results were also obtained at the array (CCV1, KYW2, AOML) and PRN15 for the launch on April 17, 1998 (Table 4). It can only be mentioned that the SAW amplitude was a factor of 3 greater than that for the launch on October 29, 1998.

Let us consider the results derived while analyzing the ionospheric effect of SAWs during the earthquake on August 17, 1999, and obtained at the array (GILB, BSHM, KATZ) for PRN 06 (Fig. 6). The average values are presented in Table 4.

In this case, the delay of the SAW response with respect to the earthquake time is 20 min. The SAW has the form of an *N*-wave with a period T of about 360 s and an amplitude A_I = 0.12 TECU, which is an order of magnitude larger than the TEC fluctuations on background days. However, it should be noted that the time interval considered is also characterized by a very low level of geomagnetic activity (–14 nT).

The amplitude of the maximal Doppler frequency shift A_F at the "reduced" frequency of 136 MHz was found to be 0.04 Hz. This corresponds to a Doppler shift of about A_F = 4 Hz at the working frequency of 13.6 MHz for the equivalent tilt sounding path.

The azimuth α and elevation angle θ of the wave vector $\mathbf{K}_t$ whose the horizontal projection is shown in Fig. 4 by the dotted line marked by $\mathbf{K}_1$ are 154° and 26°, respectively. The horizontal component and the magnitude of the phase velocity turned out to be V_h = 1307 m/s and V_t = 1174 m/s. The source coordinates at an altitude of 0 km were determined as ϕ_ω = 39.1° and λ_ω = 25.9°. The delay of "activation" of the SAW source Δt_ω with respect to the beginning of the earthquake was 12 s.

Similar results were also obtained for the earthquake on November 12, 1999. They correspond to the projection of the vector $\mathbf{K}_2$ in Fig. 4 and to the average

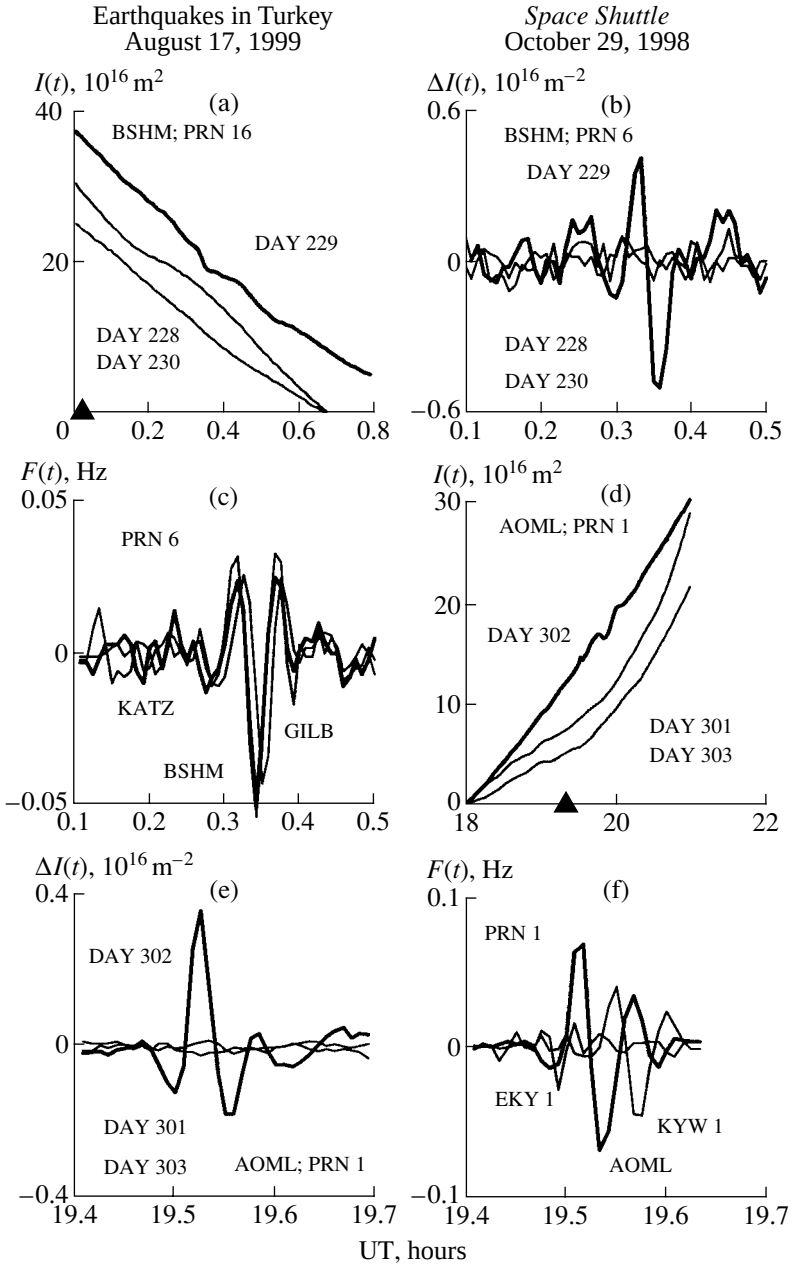

Fig. 6

data presented in Table 4. It can only be mentioned that the SAW amplitude was slightly less than that for the earthquake on August 17, 1999. With an increased level of geomagnetic activity (–44 nT), this led to a smaller "signal/noise" ratio, as compared to the earthquake on August 17, 1999. However, it does not prevent us from reliable estimation of the SAW parameters.

A comparison of the data for both earthquakes demonstrated that the SAW parameters agree well, regardless of the level of geomagnetic disturbance, the season, and the local time.

5. DISCUSSION

Now let us discuss briefly the main results and compare them to the data of other authors. As we do not have information on the dynamics and energetics of the *Proton*, *Soyuz*, and *Space Shuttle* launches nor a model of SAW emission during earthquakes, in this study we deliberately refrain from physical interpretation of the results obtained. Our goal is to get more reliable and trustworthy data implementing new possibilities provided by the global GPS monitoring.

A similarity in the SAWs detected by ionospheric soundings that are generated during rocket launches

and earthquakes should be particularly noted. It turned out that, though the characteristics and dynamics of the impact of rocket launches and earthquakes on the ionosphere are different, as are the local time, the season, and the level of geomagnetic disturbance, for all events the ionospheric response has the character of an *N*-wave. The SAW period T is equal to 270–360 s, and its amplitude exceeds the rms value of background fluctuations under quiet and moderate geomagnetic conditions by a factor of 2–5 as a minimum.

Our measurements of the period and amplitude of the SAW response agree well with the results of measuring the Doppler shifts of frequency in the HF wave range during the launches of the *Space Shuttle* LV on February 28, 1990, and April 28, 1991 [11], as well as with the corresponding estimates of the maximal shift F obtained [25, 26] for the tilt radio soundings during the launches from the Baikonur cosmodrome. They are also close to the estimates [14] obtained by radio occultation methods through sounding the ionosphere with the ultra HF wave signal from the geosynchronous satellite MARECS-B2 during the launches of the *Space Shuttle* LV on October 18, 1993 (STS-58), and February 3, 1994 (STS-60).

Two series of TEC oscillations were detected [16] during the launch of the *Space Shuttle* LV (STS-58) on October 18, 1993. The first one has an *N*-wave form with a maximal amplitude of 0.25 TECU. This also agrees with our data.

It was noted in the literature that SAWs with a similar form and a close amplitude were detected during powerful industrial explosions [7–10, 25, 27].

As was already mentioned in the Introduction, some researchers give considerably different values for the velocities of SAW propagation, up to thousands of m/s, which is beyond the limits of the speed of sound at the heights of SAW propagation in the atmosphere. According to the data presented in review [28], the velocity of propagation of the SAW ionospheric response varied from 600 to 1670 m/s as recorded during the *Apollo* rocket missions.

It was hypothesized in [29] that the shock wave associated with a rocket flight separates at an altitude of about 160 km in the ionosphere into an ion-acoustic mode (with a velocity of up to 1.3 km/s) and a normal acoustic mode (with a velocity as high as 500 m/s). The difference in propagation velocities of the first and second disturbances was observed during the *Apollo 14* and *Apollo 15* launches at one and the same distance of 1440 km from the launch site. Differences in atmospheric conditions and trajectories of wave propagation due to seasonal ionospheric variations can be responsible for this.

The observations of long-period waves [30] over the incoherent scatter radar at Arecibo were described for the period of the *Space Shuttle* (STS-4) launch on June 27, 1982. The group velocity of the wave propagation was found to be 600–700 m/s at a large distance (as far as 1000 km) from the path. According to GPS measurements [16], the phase velocity of the SAWs is on the order of 1000–1300 m/s at ionospheric heights.

A common drawback of the well-known methods used for determination of the SAW phase velocity is their need for a predetermined time of the rocket launch. This follows from the fact that the velocity is calculated from the SAW delay with respect to the launch time under the assumption of constant velocity along the propagation path, and this assumption is far from reality. Moreover, essentially, only the horizontal component of the phase velocity V_h was determined in these studies. At different elevation angles of the wave vector $\mathbf{K}_t$, the velocity V_h is associated with considerably different values of the magnitude of the phase velocity V_t.

With the method proposed in this study, one has the possibility to determine the angular characteristics of the wave vector $\mathbf{K}_t$ and, correspondingly, estimates of V_t. According to our data (Tables 3, 4), the elevation angle of the SAW wave vector ranges from 30° to 60° and the SAW phase velocity varies from 900 to 1200 m/s. We determine the phase velocity of propagation of the line of equal TECs at the height of the ionospheric F-region maximum. This region contributes most to variations of the total electron content between the receiver and the GPS satellite, and the sensitivity of the method is maximal there. As V_t is close to the speed of sound at these altitudes [7, 14], this allows one to identify the sound nature of the TEC disturbance.

The location of SAW sources as calculated without refraction correction corresponds to a path segment at a distance of no less than 700–900 km from the launch site for the *Proton* or *Soyuz* LVs (Figs. 1, 2) and no less than 200–500 km for the *Space Shuttle* LV (Fig. 3). This agrees with the delay Δt_ω of the source "activation", which is 195–300 s for the *Proton* and *Soyuz* LVs and 195–230 s for the *Space Shuttle* LV. It can be seen from our data that the calculated location of the SAW source during rocket launches does not coincide with the position of the launch site. At the same time, the coordinates of the source are in rather good agreement with those of the horizontal projections of the LV trajectories (Figs. 1–3).

The data from infrasound measuring arrays on the northeastern coast of the United States were analyzed in [31]. Strong acoustic signals were observed from the launch and reentry areas of the *Saturn 5* LV. The authors recognize three types of signals. The first type was associated with early signals, whose arrival time corresponded to supersonic values of their velocity, equal to 500–1000 m/s. The second type represented normal signals with the group velocity approximately equal to the normal speed of sound in the air. The last type included late signals with subsonic velocities ranging from 190 to 240 m/s. It was suggested in [31] that the so-called "early" signals during rocket launches are caused by the SAWs generated during the reentry of the

first stage at distances of more than 500 km from the launch site.

However, our data, which were obtained from comparing the estimates of the velocities V_h, V_t, and V_a, as well as of the azimuth α of the SAW wave vector **K**, are in better agreement with a mechanism asserted in [6, 14, 16, 26]. The authors of these studies believe that the SAWs are generated when a rocket moves nearly horizontally along the acceleration segment of its trajectory in the lower atmosphere at heights of 100–130 km with the operating engine. The rocket passes this segment with a supersonic velocity at the 100th–300th s of its flight at a distance of more than 500 km from the launch site. As soon as the rocket ascends to an altitude of about 100 km, the SAW source is "activated."

The location of the SAW source calculated without refraction correction approximately corresponds to the earthquake epicenter. Our data agree with the existing ideas that the shock–acoustic waves are generated due to forcer-like motions of the Earth's surface in the epicentral zone of earthquakes [3, 32].

CONCLUSIONS

The authors hope that this study will contribute to a better understanding of the physical processes that occur in the Earth's atmosphere during rocket flights along the initial segment of the trajectory, as well as during earthquakes. Moreover, it will help to find more reliable signal indications of technogenic effects, which are necessary for constructing an effective global radiophysical system for detection and localization of these effects on the basis of processing the data from the international network of two-frequency receivers of the GPS–GLONASS navigation systems.

ACKNOWLEDGMENTS

The authors thank E.A. Ponomarev, V.V. Evstaf'ev, P.M. Nagorskii, N.N. Klimov, A.M. Uralov, and A.D. Kalikhman for their interest in this study, useful advice, and active participation in discussions. This study was supported by the Russian Foundation for Basic Research (grant no. 99-05-64753); by the Program of support of leading scientific schools of the Russian Federation, grant no. 00-15-98509; and by the Ministry of Science, Higher Education, and Technical Policy of the Russian Federation (Minvuz), grant 1999, with B.O. Vugmeister as the principal investigator.

REFERENCES

1. Calais, E. and Minster, J.B., GPS Detection of Ionospheric Perturbations Following the January 1994, Northridge Earthquake, *Geophys. Res. Lett.*, 1995, vol. 22, p. 1045.
2. Golitsyn, G.S. and Klyatskin, V.I., Oscillations in the Atmosphere Generated by Motions of the Earth's Surface, *Izv. Akad. Nauk SSSR, Ser. Fiz. Atmosf. i Okeana*, 1967, vol. 111, no. 10, p. 1044.
3. Orlov, V.V. and Uralov, A.M., Response of the Atmosphere to an Earthquake-Generated Rayleigh Wave, *Issledovaniya po geomagnetizmu, aeronomii i fizike Solntsa* (Studies in Geomagnetizm, Aeronomy, and Solar Physics), Moscow: Nauka, 1987, no. 78, p. 28.
4. Row, R.V., Acoustic-Gravity Waves in the Upper Atmosphere due to a Nuclear Detonation and an Earthquake, *J. Geophys. Res.*, 1967, vol. 72, no. 5, p. 1599.
5. Ekologicheskie problemy i riski vozdeistvii raketno-kosmicheskoi tekhniki na okruzhayushchuyu prirodnuyu sredu. Spravochnoe posobie (Ecological Problems and Risks of Impact of the Rocket-Space Facilities on the Environment: A Handbook), Moscow: Ankil, 2000, p. 640.
6. Nagorskii, P.M., Rocket-Induced Inhomogeneous Structure of the Ionosphere F-Region, *Geomagn. Aeron.*, 1998, vol. 38, p. 100.
7. Fitzgerald, T.J., Observations of Total Electron Content Perturbations on GPS Signals Caused by a Ground Level Explosion, *J. Atmos. Solar–Terr. Phys.*, 1997, vol. 59, p. 829.
8. Calais, E., Minster, B.J., Hofton, M.A., and Hedlin, M.A.H., Ionospheric Signature of Surface Mine Blasts from Global Positioning System Measurements, *Geophys. J. Int.*, 1998, vol. 132, p. 191.
9. Afraimovich, E.L., Varshavskii, I.I., Vugmeister, B.O., *et al.*, The Effect of Ground Industrial Explosions on Doppler and Angular Characteristics of Radio Signal Reflected from the Ionosphere, *Geomagn. Aeron.*, 1984, vol. 24, p. 322.
10. Blanc, E. and Jacobson, A.R., Observation of Ionospheric Disturbances Following a 5-kt Chemical Explosion. 2. Prolonged Anomalies and Stratifications in the Lower Thermosphere after Shock Passage, *Radio Sci.*, 1989, vol. 24, p. 739.
11. Jacobson, A.R. and Carlos, R.C., Observations of Acoustic-Gravity Waves in the Thermosphere Following Space Shuttle Ascents, *J. Atmos. Solar–Terr. Phys.*, 1994, vol. 56, p. 525.
12. Mendillo, M., The Effects of Rocket Launches on the Ionosphere, *Adv. Space Res.*, 1981, vol. 1, p. 275.
13. Mendillo, M., Modification of the Ionosphere by Large Space Vehicles, *Adv. Space Res.*, 1982, vol. 2, p. 150.
14. Li, Y.Q., Jacobson, A.R., Carlos, R.C., *et al.*, The Blast Wave of the Shuttle Plume at Ionospheric Heights, *Geophys. Res. Lett.*, 1994, vol. 21, p. 2737.
15. Klobuchar, J.A., Real-Time Ionospheric Science: The New Reality, *Radio Sci.*, 1997, vol. 32, p. 1943.
16. Calais, E. and Minster, J.B., GPS Detection of Ionospheric Perturbations Following a Space Shuttle Ascent, *Geophys. Res. Lett.*, 1996, vol. 23, p. 1897.
17. Afraimovich, E.L., Kosogorov, E.A., and Plotnikov, A.V., Detection of Acoustic Shock Waves Generated during Rocket Launches by GPS Arrays, in *Trudy VI mezhdunarodnoi nauchno-tekhnicheskoi konferentsii "radiolokatsiya, navigatsiya, svyaz'," Voronezh, 25–27 aprelya 2000 g.* (Proc. VI Intern. Conf. "Radiolocation, Navigation, Communication," Voronezh, April 25–27, 2000), vol. 1, p. 462.

18. Afraimovich, E.L., Kosogorov, E.A., Palamarchouk, K.S., *et al.*, The Use of GPS Arrays in Detecting the Ionospheric Response during Rocket Launchings, *Earth, Planets, and Space*, 2000, vol. 52, p. 1061.
19. Hofmann-Wellenhof, B., Lichtenegger, H., and Collins, J., *Global Positioning System: Theory and Practice*, New York: Springer, 1992, p. 327.
20. Davies, K., *Ionospheric Radio Waves*, London: Blaisdell, 1969. Translated under the title *Radiovolny v ionosfere*, Moscow: Mir, 1973, p. 502.
21. Bertel, L., Bertin, F., and Testud, J., De la Mesure du Contenu Electronique Integre Appliquee a l'Observation des Ondes de Gravite de Moyenne Echelle, *J. Atmos. Solar–Terr. Phys.*, 1976, vol. 38, p. 261.
22. Afraimovich, E.L., Terechov, A.I., Udodov, M.Yu., and Fridman, S.V., Refraction Distortions of Transionospheric Radio Signals Caused by Changes in a Regular Ionosphere and by Traveling Ionospheric Disturbances, *J. Atmos. Solar–Terr. Phys.*, 1992, vol. 54, p. 1013.
23. Mercier, C. and Jacobson, A.R., Observations of Atmospheric Gravity Waves by Radio Interferometry: Are Results Biased by the Observational Technique?, *Ann. Geophys.*, 1997, vol. 15, p. 430.
24. Afraimovich, E.L., Palamartchouk, K.S., and Perevalova, N.P., GPS Radio Interferometry of Traveling Ionospheric Disturbances, *J. Atmos. Solar–Terr. Phys.*, 1998, vol. 60, p. 1205.
25. Nagorskii, P.M., *Doctoral (Phys.-Math.) Dissertation*, Tomsk: Tomsk State Univ., 1998.
26. Nagorskii, P.M., Analysis of Short-Wave Radio Signal Response to a Disturbance of Ionosphere Plasma Caused by Acoustic Shock Waves, *Izv. Vyssh. Uchebn. Zaved., Radiofiz.*, 1999, vol., p. 36.
27. Jacobson, A.R., Carlos, R.C., and Blanc, E., Observation of Ionospheric Disturbances Following a 5-kt Chemical Explosion. 1. Persistent Oscillation in the Lower Thermosphere after Shock Passage, *Radio Sci.*, 1988, vol. 23, p. 820.
28. Karlov, V.D., Kozlov, S.I., and Tkachev, G.N., Large-Scale Disturbances in the Ionosphere Excited during the Flight of a Rocket with Operating Engine, *Kosm. Issled.*, 1980, vol. 18, p. 266.
29. Arendt, P.R., Ionosperic Undulations Following "Appolo-14" Launching, *Nature*, 1971, vol. 231, p. 438.
30. Noble, S.T., A Large-Amplitude Traveling Ionospheric Disturbance Excited by the Space Shuttle during Launch, *J. Geophys. Res*, 1990, vol. 95, p. 19037.
31. Kaschak, G., Donn, W.L., and Fehr, U., Long-Range Infrasound from Rockets, *J. of the Acoust. Society of America*, 1970, vol. 48, no. 1(1), p. 12.
32. Rudenko, G.V. and Uralov, A.M., Calculation of Ionospheric Effects due to Acoustic Radiation from an Underground Nuclear Explosion, *J. Atmos. Terr. Phys.*, 1995, vol. 57, p. 225.